Journal of Materials and Engineering Structures

Research Paper

Appropriate sample size and effects of microscopic parameters on the shear strength and strain localisation of 2D cohesive-frictional granular assemblies

Trung-Kien Nguyen [a,*], Thanh-Trung Vo [b, c], Nhu-Hoang Nguyen [a]

[a] *Faculty of Building and Industrial Construction, Hanoi University of Civil Engineering, 55 Giai Phong road, Hanoi, Vietnam.*

[b] *School of Transportation Engineering, Danang Architecture University, 566 Nui Thanh street, Danang city, Vietnam*

[c] *Office of Research Administration, Danang Architecture University, 566 Nui Thanh street, Danang city, Vietnam*

ARTICLE INFO

Article history :

Received : 17 April 2023

Revised : 3rd July 2023

Accepted : 1st September 2023

Keywords:

DEM

Granular materials

Microscopic effects

Strain localisation

ABSTRACT

Granular materials are made up of smaller particles, manifestation of microstructure results in a macroscopic response of granular material. Understanding the overall mechanical behaviour from microscopic parameters is one of the main challenges in many engineering fields including civil engineering. When modelling this kind of material by Discrete Element Model (DEM) using idealized circular grains, the effects of appropriate sample size and microscopic parameter changes have been a crucial subject. Previous research has primarily relied on the case of purely frictional granular materials. In this paper, we use DEM to investigate the appropriate sample size and the relationship between microscopic parameters and the macroscopic responses of cohesive-frictional granular assemblies by performing a series of biaxial tests. Our findings indicate that a minimum number of particles is required to balance between mechanical behaviour and computing time. In addition, through extensive parametric studies, the paper explores the impact of factors such as interparticle bonds, intergranular friction coefficients, and initial void index on the overall shear behaviour of granular assemblies. Also, the result reveals a strong correlation between shear band formation and the break field of cohesive contact (static variable) and the translations and rotations of grains (kinematic variable).

1 Introduction

Granular materials are present in all aspects of life and are commonly found in civil engineering applications. In this domain, most construction materials are of discrete structure, heterogeneous and anisotropic characteristics such as granular soil or concrete. Granular materials are made of particles at smaller scales. When the materials are subjected to loading, their particles interact and govern the overall behaviour of granular materials. Changes in microscopic evolution lead to

* *Corresponding author. Tel.: +84 907141086*
E-mail address: kiennt3@huce.edu.vn

e-ISSN: 2170-127X,

RESEARCH REVIEW of Sciences and Technologies

macroscopic changes in the behaviour of granular materials [1-6]. Trying to catch as realistically as possible the behaviour of materials from particle interactions is of real challenge in numerical modelling.

Modelling the behaviour of granular material in civil engineering involves understanding and simulating the physical properties and interactions of the individual particles that make up the material. This can include factors such as particle shape, size, and density, as well as the forces that act upon the particles, such as friction and interaction forces. There are various numerical methods and models available for this purpose, including Discrete Element Method (DEM), Finite Element Method (FEM), Material Point Method (MPM), or Smoothed-particle hydrodynamics (SPH) [7-11]. These methods can be used to analyse and predict the behaviour of granular materials in a wide range of civil engineering applications, such as soil mechanics or related geotechnical structures. Finite Element Method has been used extensively in the past to model the behaviour of granular materials, but it can be challenging to accurately describe the discrete, heterogeneous, and anisotropic nature of granular materials in a simple constitutive law. At the end of the 1970s, Cundall and Struck [12] pioneered the use of Discrete Element Method (DEM) in modelling the behaviour of granular materials. Since then, the DEM has been widely used and proven to be a highly efficient tool for investigating the origin of the behaviour of granular materials [13-16].

One of the main challenges in modelling the behaviour of granular material by DEM is the sample size (or number of particles) used in the model [17, 18]. The number of particles used in DEM depends on the specific application and the level of detail required in the simulation. In general, a larger number of particles will result in a more detailed and accurate simulation, but it also greatly increases the computational cost. Thus, the number of particles used in a simulation should be justified by the requirements of the problem, the computational resources, and the simulation goals. In our case, this should be carefully judged between computer performance and the mechanical behaviour of the model. Finding the right balance between computational efficiency and accurately simulating the mechanical behaviour of the granular material is crucial. In soil mechanics and geotechnical engineering, the biaxial test is used to investigate the behaviour of geomaterial under laboratory conditions, but to the author's best knowledge, determining the appropriate sample size for a 2D biaxial simulation using DEM with idealized circular grains is still elusive except for the reference [19]. However, in this paper, Kuhn and Bagi [19] only considered the case of purely frictional granular assembly. True in nature, granular materials are usually found with the existence of cohesive interaction parts, which greatly affect the overall response of granular materials. Moreover, in DEM, interactions between particles are modelled using forces and relative displacement, and macroscopic response, such as stress, is calculated based on these interactions. Thus, the overall behaviour of granular materials is largely determined by these interactions. Additionally, the initial state of the granular material can also affect its behaviour. It is therefore important to investigate how changes in microscopic parameters influence the macroscopic responses of granular materials.

When studying the stability of structures made of granular materials, it is frequently observed that the failure of granular materials structures is due to a concentration in a small area, known as strain localisation [10, 20-23]. Strain localisation refers to the phenomenon in which a small region of granular material (called localised region) undergoes a much larger deformation than the surrounding material. The strains in the localised region can become very large, leading to the formation of shear bands, which are narrow regions of intense deformation and thus can cause the material to fall in a localised manner and greatly affect the integrity of the structure. This phenomenon has been recognised in both numerical/experimental laboratory tests and in geotechnical structures [1, 24-27]. Despite being widely recognized, the behaviour of granular materials under strain localisation is complex and not yet fully understood, making it a preferred area of research in the field of geomechanics. Since granular materials are made up of smaller particles, strain localisation in granular materials can result in a variety of microscopic changes within the material. The strong manifestation of microstructure results in a macroscopic response of granular material including strain localisation. Establishing the link between micro- and macro-scales information has been the subject of numerous research studies.

To deal with these questions from a macro-micro point of view, in this present research, we report the effects of microscopic properties on the shear behaviour of granular assembly through a series of biaxial tests using discrete element modelling. By varying a broad range of values of microscopic parameters, the macroscopic behaviour is analysed and discussed along with the changes in microscopic parameters. This paper is organized as follows: Section 2 briefly introduces the DEM basic principle, model preparation, and simulation procedure, and a series of biaxial tests. Section 3 presents numerical results along with discussions that focus on the microscopic properties induced changes in macroscopic responses. Finally, in Section 5, we summarize our main conclusions and recommendation for future work.

2 DEM simulation procedure

In DEM, the granular material is represented as a collection of discrete particles that interact with each other based on their physical properties. In the current model, we consider grains as 2D circular particles. Circular grains are assumed as rigid bodies and interact via interaction law. Their interactions involving normal (f_n) and tangential (f_t) components. The normal force is composed of normal elastic force (f_{el}) and normal cohesive force (f_c) such as $f_n = f_{el} + f_c$. The cohesive force is defined in proportion to the isotropic compression stress of the granular assembly $f_c = c \cdot (\sigma_0 \cdot a)$ where c is the cohesive level, a is the mean diameter of granular assembly and σ_0 is isotropic compression stress [8, 18]. The tangential force is followed and limited by Coulomb friction, $|f|_t \leq \mu f_n$ [8, 28]. The overlapping region of two grains in contact δ (Fig. 1) is thus small compared to particle size (R_i, R_j). Rolling resistance is not taken into account in the current model. The simulations reported in this study are performed by 2D-in house DEM code, named PBC2D which is originally developed by [29] and then improved by the authors in recent works [16, 30].

The sample preparation process includes the following steps: (1) creating granular assemblies with uniform grain size distribution. In this step, the number of particles is varied systematically; (2) apply isotropic compression loading to the granular sample. In this second step, different values of stiffness number, friction coefficient, and cohesive level are used.

2.1 Biaxial loading test

From the isotropic stress level, the sample is performed biaxial loading with displacement controlled on the top and bottom surface while lateral confining stress is kept constant and equal to isotropic compression stress. Multi-periodic boundary conditions are applied to the edges of granular samples [31]. The principle of biaxial loading and grain-scale interaction law is schematized in Fig. 1

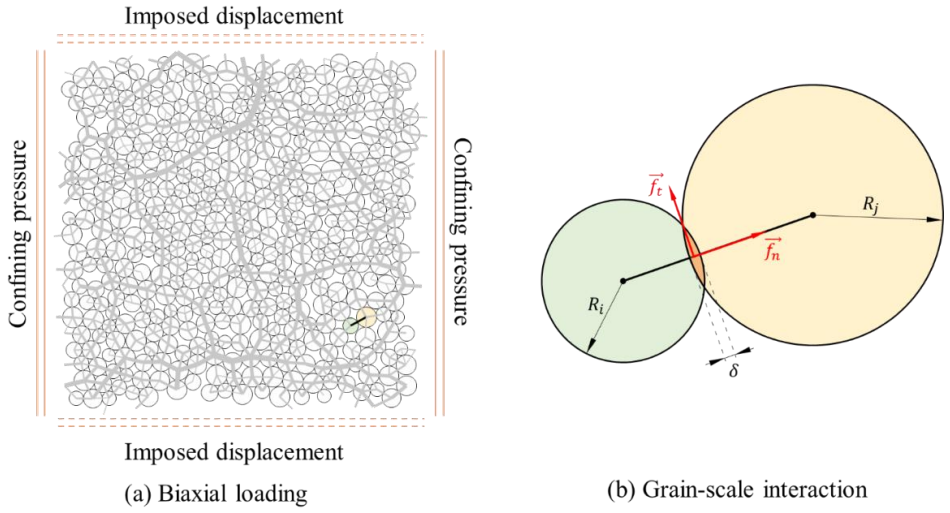

Fig. 1 – Biaxial loading principle and grain-scale interaction law

2.2 Macroscopic parameters

The overall stress tensor of granular assembly is calculated by homogenized formula $\sigma = \frac{1}{V}\sum_c \vec{f_c} \otimes \vec{l}$, where $\vec{f_c}$ is contact force and $\vec{l}$ is the branch vector joining the centers of two particles in contact. V is the volume (in 2D case) of granular assembly and c is the contact list. The operator $\otimes$ denotes the tensorial product of two vectors.

In the case of 2D biaxial test, the deviatoric stress is determined by $q = \sigma_1 - \sigma_2$ where σ_1 and σ_2 are axial stress and lateral confining pressure, respectively. The axial and volumetric strain are defined as $\varepsilon_{11} = \frac{h_0 - h}{h_0}$ and $\varepsilon_v = \frac{V_0 - V}{V_0}$ where h, V are the height and volume of granular assembly at the current time step and h_0, V_0 are the initial height and volume. Soil mechanics convention is adopted: $\varepsilon_{11} > 0$, $\varepsilon_v > 0$ means axial and volume in compression.

3 Numerical results: microscopic parameter affecting macroscopic behavior

3.1 Determination of the appropriate number of particles (npa)

The appropriate number of particles (npa) in a Discrete Element Method (DEM) simulation is crucial for achieving the right balance between the computational performance and the mechanical behaviour. In practice, the number of particles used in a simulation is often determined through a process of trial and error, where the simulation is first run with a relatively low number of particles, and then the results are compared with other simulations. The reliability of the results can be evaluated by statistical analysis. The number of particles can then be increased until the simulation results reach an acceptable degree of accuracy.

To this matter, we perform an analysis in varying the number of particles in the granular assembly. Six sizes of granular samples were generated with npa equals 400, 900, 2500, 5625, 8100, and 10000 particles. Three granular assemblies (i.e. realizations R01, R02, R03) were prepared for each sample size. A total of 3x6=18 samples have been generated with the same microscopic parameters (see Table 1 for details). Between three realizations of similar size (i.e. number of particles), we generate random different grain size distribution while respecting uniform law and the ratio between maximum and minimum grain size is kept constant and equal $r_{max}/r_{min} = 5/3$. After isotropic compression, all samples were in a similar dense state and then subjected to compression biaxial loading. Normalized deviatoric stress versus vertical strain was extracted and represented in Fig. 2. In each sub-figures of Fig. 2, we present the stress-strain curve for each realization and the average of them. Typical curves of deviatoric stress are obtained in all cases. The value of normalized deviatoric stress increases rapidly to the peak corresponding to the maximum strength of granular assembly, and then decreases to reach a plateau.

Table 1 - Characteristic of samples

No.	Samples	npa	$\kappa = k_n/(\sigma_0 \cdot a)$	μ	c	Initial state
1	S400-R01	400	1000	0.5	1	Dense
2	S400-R02					
3	S400-R03					
4	S900-R01	900	1000	0.5	1	Dense
5	S900-R02					
6	S900-R03					
7	S2500-R01	2500	1000	0.5	1	Dense
8	S2500-R02					
9	S2500-R03					
10	S5625-R01	5625	1000	0.5	1	Dense
11	S5625-R02					
12	S5625-R03					
13	S8100-R01	8100	1000	0.5	1	Dense
14	S8100-R02					
15	S8100-R03					
16	S10000-R01	10000	1000	0.5	1	Dense
17	S10000-R02					
18	S10000-R03					

It can be seen that the macroscopic response of a granular assembly becomes smoother and the scattering in stress decreases with increasing the number of particles. When the number of particles is small, little change in the grain re-arrangement can result in a large change in stress due to variation in interaction forces and grain displacement. From a

sufficient number of particles, the stress-strain behaviour is stable enough to be mechanically representative. In the present simulations, a well-marked peak in the stress-strain curve is obtained when the number of particles exceeds 8100.

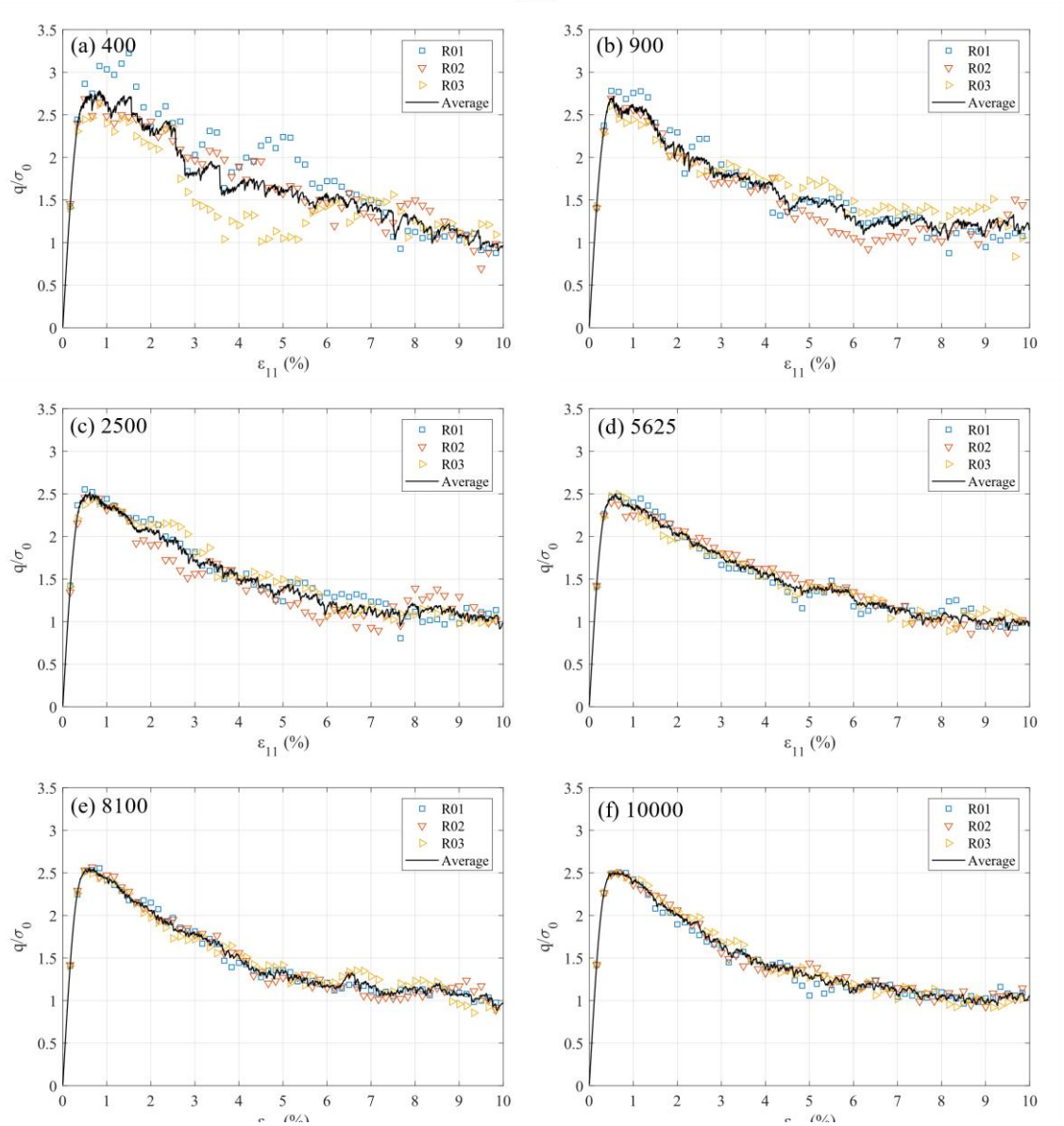

Fig. 2 – Numerical result: stress-strain behaviour with respect to number of particles

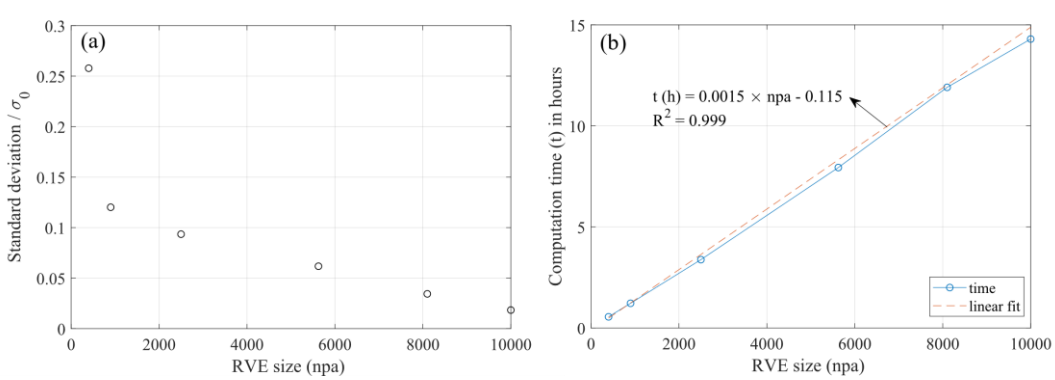

Fig. 3 – Standard deviation of shear strength and computation time varies with sample size

To confirm the visual inspection, we compute the standard deviation (sd) of each sample size and plot it in Fig. 3 (a). The standard deviation decreases with increasing number of particles but becomes less significant with exceeding 8100 particles ($sd < 0.05$). In fact, the number of grains in the simulation has a significant impact on the computation time. Fig. 3 (b) gives comparative information on computation time between the simulations. For each sample size, the time computation represented in the figure is the mean value of three realizations. As the number of particles increases, the computation time seems to increase linearly. To achieve a good balance between the accurate mechanical behaviour of the granular assembly and reasonable computation time, the number of particles must be carefully selected. In our study, we found that using 8100 particles provides a good balance between these two factors. Therefore, we use 8100 particles in the remaining simulations of the paper.

3.2 Influence of intergranular friction coefficient (μ) on the behaviour of granular assembly

Contact friction is an important factor that can affect the mechanical response of granular assembly. In the DEM simulation, intergranular friction is represented by a coefficient that controls sliding contact thanks to Coulomb inequality $|f|_t \leq \mu f_n$. As a result, the maximum tangential force changes with the intergranular coefficient of friction. Consequently, the overall stress of the granular sample, which is computed by force interactions, must be influenced. In this section, we vary the coefficient of intergranular friction μ while keeping the other parameters constant. It was set as $\mu = 0.3, 0.5, 0.7$. The evolutions of normalized deviatoric stress versus axial strain are then shown in Fig. 4.

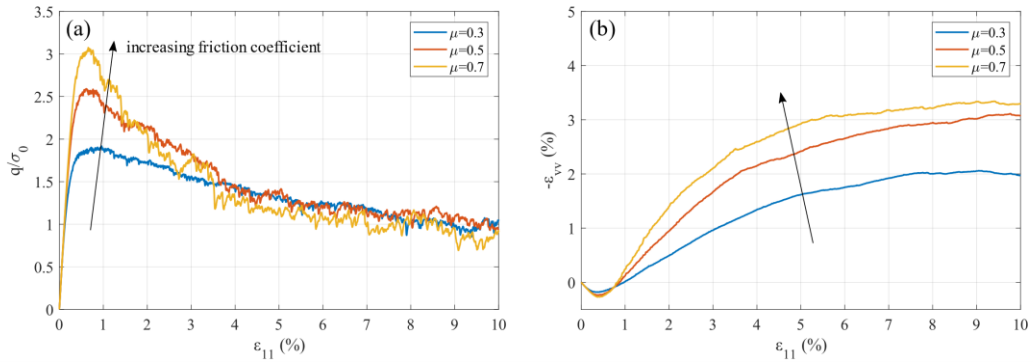

Fig. 4 – Numerical result: intergranular friction coefficient study

The results indicate that as μ increases, the peak stress becomes larger and more pronounced. For large deformations $\varepsilon_{11} > 5\%$, the intergranular friction coefficient μ does not influence much the evolution of the macroscopic stress. Indeed, in large deformations, the shape of the grains plays a much more important role than the coefficient of intergranular friction μ [32, 33]. It therefore similar critical resistance was found. Regarding the volumetric strain evolution, the contracting and dilating phases are both more pronounced with the higher value of μ.

3.3 Influence of inter-particle cohesive level (c)

Besides friction, cohesion is another important factor that affects the mechanical response of granular materials. In order to shed light on the role of the cohesion level on the macroscopic behaviour of the material, we seek to vary the values of cohesive level c. The cohesive level compared cohesive force f_c to average force due to confining pressure as $f_c = c \cdot (\sigma_0 \cdot a)$. If $c \ll 1$, the force due to confinement plays a main role and cohesive effects are negligible.

Using different values of c ($c = 0.5, 1.0, 1.5$), a parametric study has been conducted. The results in Fig. 5 show a strong influence of this parameter. As c increases, the peak stress increases and is reached for slightly larger axial strains ε_{11}. This observation explains the influence of c on the strength of the material: a larger value of c produces a higher material strength. This corresponds to the maximum strength of the material reached and the peak at larger axial strains if c increases. Classically in soil mechanics, the Mohr-Coulomb criterion is usually used to evaluate the macroscopic characteristic of soil. Additional extensional biaxial tests were performed in order to deduce the two parameters (C, φ) of Morh-Coulomb criterion ($\tau = \sigma_n \cdot tan\varphi + C$) (not shown here for lack of space). Thanks to Mohr's circles the values of C and φ for three considered cases are obtained as follows: $C = 0.3 \cdot \sigma_0 \cdot c$ and $\varphi \approx 25^0$. It is expected that the macroscopic cohesion increases with c.

Indeed, macroscopic cohesion comes mainly from the microscopic bonds. The internal friction angle does not depend on c. This result is logical because μ is identical in all simulations. A slight increase in φ with c is simply explained by increasing the number of coordination with the cohesive level c. Regarding volumetric strain evolution, the result shows that by increasing the cohesive level, the material becomes more contracting in the first phase and the dilatancy angle is relatively larger, as shown in Fig. 5(b).

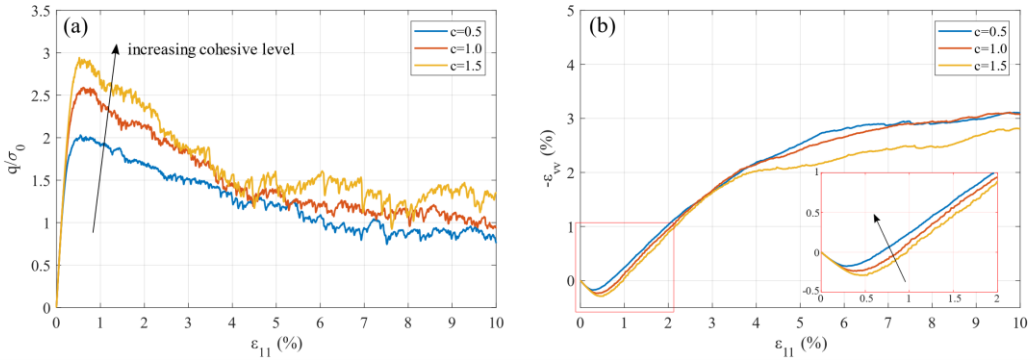

Fig. 5 – Numerical result: inter-particle cohesive level study

3.4 Influence of initial void index

The initial void index, also known as the initial porosity, is a measure of the initial space or voids present in a granular material. It is defined as the ratio of the volume of voids to the total volume of the material. The initial void index can have a significant impact on the behaviour of granular materials under loading conditions, including the phenomenon of strain localisation [26, 34]. In this parametric study, four samples with different initial void index ratios have been generated and then subjected to biaxial loading. The mechanical responses of these samples are shown in Fig. 6. The arrows classify the curves according to the increasing initial compactness (decrease of initial void ratio) that is obtained after the isotropic compression. Here we obtain the typical range of behaviour of granular soils. Concerning stress, the peak increases with the density of the sample. A loose sample does not show a peak. For large strains, all samples tend to have the same stress level. These simulations confirm the theory of the critical state: the internal state of the material approaches a certain state called "the critical state", independently of the initial state when it is subjected to large deformations. If the phenomenon of strain localisation is observed, the critical state of the material lies within the shear bands, and the sample is dominated by these narrow bands. Simultaneously with the stresses, the kinematic evolutions are also very typical. Dense samples represent contracting first and then dilating behaviours, while loose samples are purely contracting.

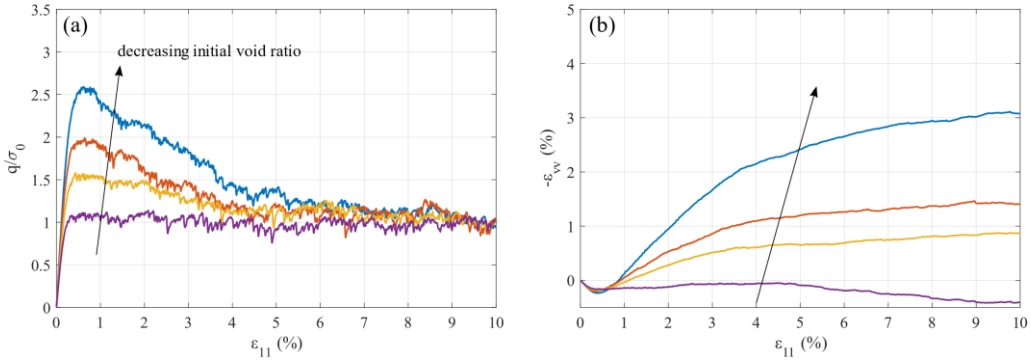

Fig. 6 – Numerical result: initial void index study

4 Strain localisation in 2D granular sample

As strain localisation is frequently observed when granular materials undergo large strain and is recognised as one of the main sources that trigger failure, in this section, we aim at bridging the correlation between macroscopic concentration of

deformation (known as strain localisation) and microscopic changes inside granular samples. To measure the occurrence and propagation of strain localisation in the above numerical test on granular assembly, we compute the local shear intensity over the sample. The local strain is determined as follows: the granular assembly is divided into polygonal void cells based on the contacting grains. The strain of polygonal void is evaluated from the translations of grains as suggested by [35, 36]. In Fig. 7 below, the strain localisation occurred inside granular assembly is assessed in terms of both local static and kinematic variables.

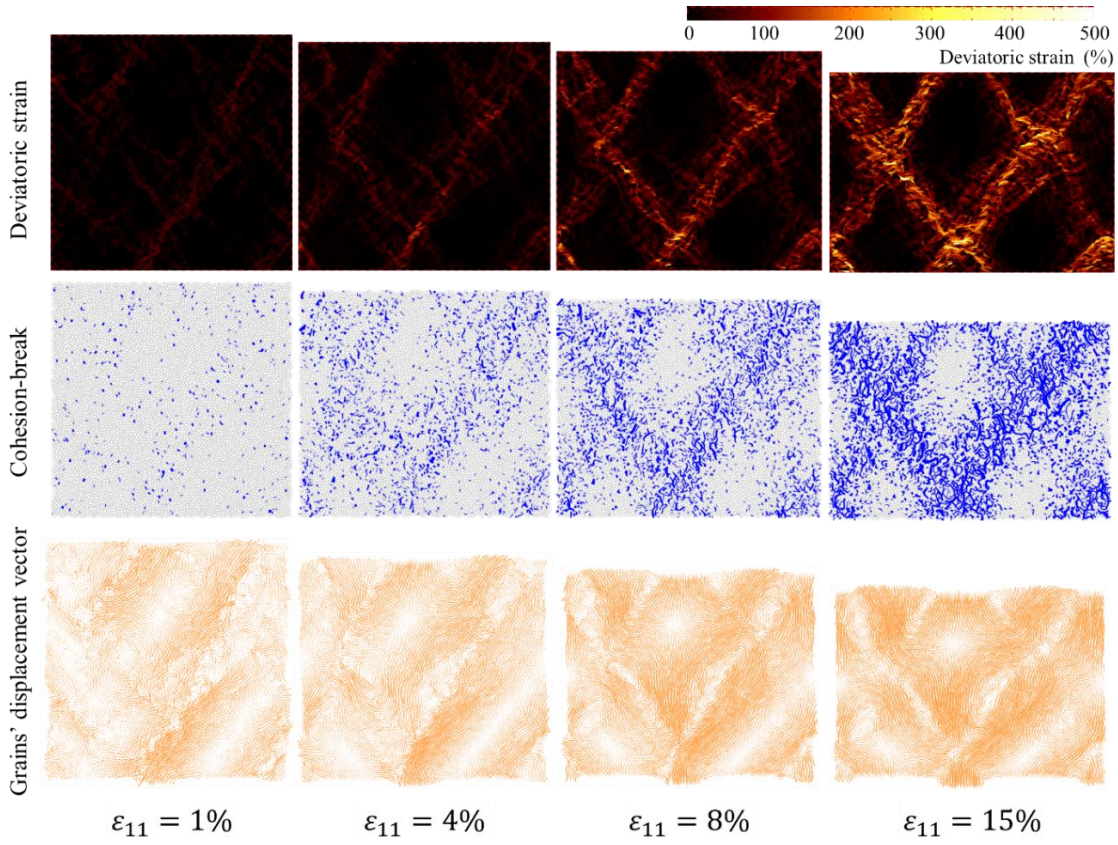

Fig. 7 – Deviatoric strain in, cohesion-break field and grain's displacement vector in S8100-R01

Taking S8100-R01 as a reference, Fig. 7 (first row) shows the evolution of shear intensity in terms of deviatoric strain with axial strain. It is evident that the shear bands (SB) become more and more visible after the onset which corresponds to the peak in stress-strain curve. At the peak, even the shear band is not yet visible, a first hint is clearly shown in this figure and allows prediction of future shear band locations. When all SB are fully formed, we obtained two periodic-"crossing" shear bands (herein the word "crossing" is used to indicate the intersection of SB). In the second row of Fig. 7, we show the force chains map of contact without cohesion. As a remainder, all contacts were initially cohesive, thus this map corresponds to contacts that lose cohesion. Hereafter, this map is referred to cohesion-break field. The last row of Fig. 7 presents the displacement vector field of particles. It is determined by computing the relative translation of particles in the vertical and horizontal axis compared to the initial state. Comparing the three rows in Fig. 7 shows a good correlation in terms of strain localisation between grains' kinematic (displacement vector field – third row) and static variable (cohesion-break field – second row). All three rows of figures reveal a same story: soon at the peak in stress-strain response, heterogeneous deformation field is obtained which corresponds to the increasing displacement field, especially in future localised zones. The formation of shear bands, which can cause failure, becomes clearer as strain increases, notably from 4 percent of vertical shortening of the whole sample. The shear zones are formed in several bands that run across the sample which is also evident in the force chains network. Contacts that lose cohesion are also concentrated in the shear localised zones even some others are found outside. This is a remarkable feature and leads to confirming the correlated information between the shear localised and both kinematic and static variables of granular assembly and is in line with experimental observations by [25, 37].

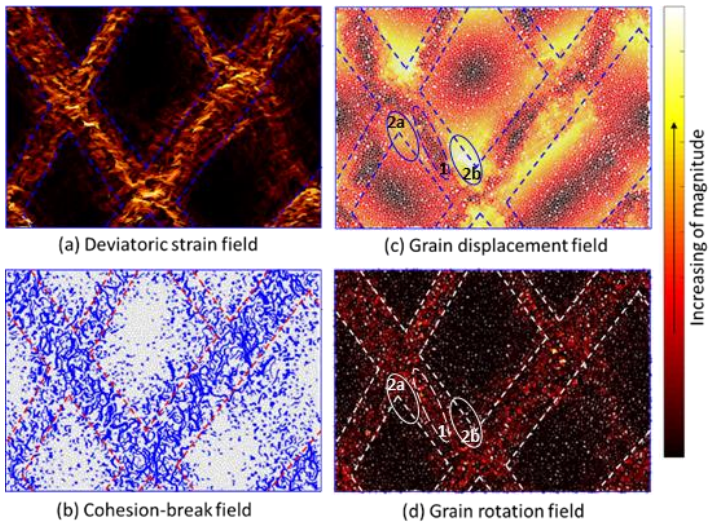

Fig. 8 – Strain localisation correlation in S8100-R01 at 15% of axial shortening

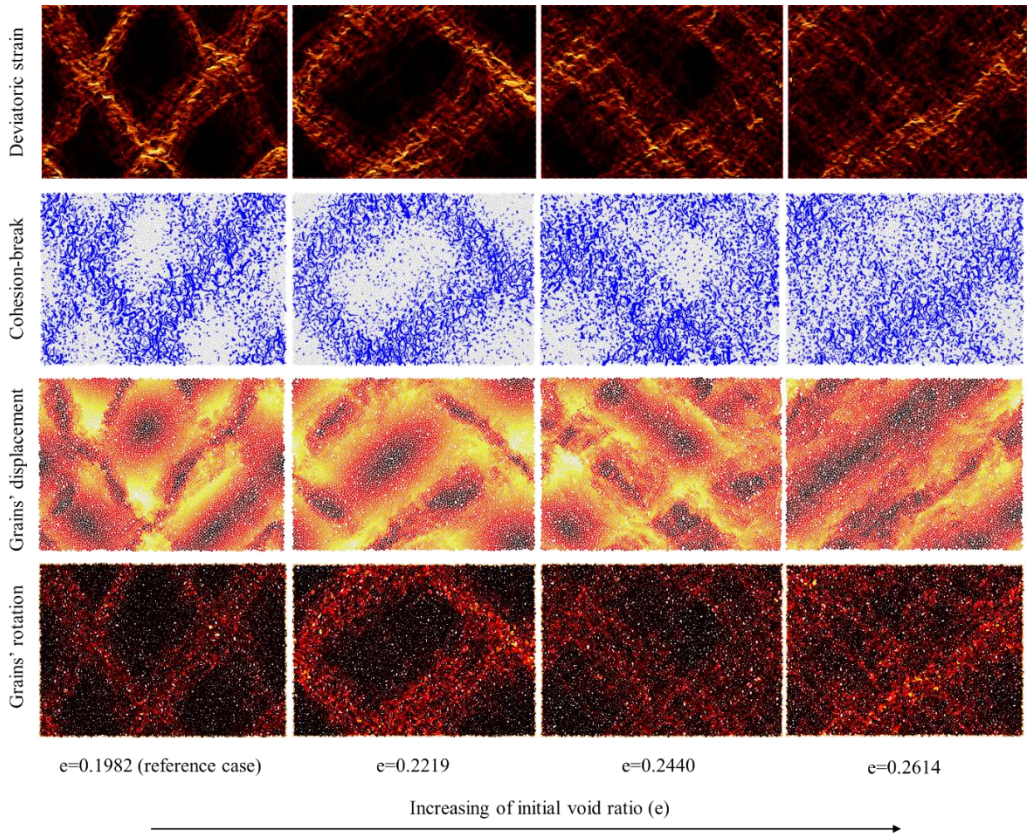

Fig. 9 – Strain localisation: Initial void ratio study

A more detailed comparison between strain localisation viewed by the deviatoric strain field and micromechanical features at the end of the simulation ($\varepsilon_{11} = 15\%$), interesting correlations are revealed in Fig. 8 when we take a closer look at the localised zones bounded by dashed lines. While the formation of SB corresponds to the increase of displacement field, remarkably it can be seen that the core of SB has almost negligible grain displacement (zone 1 of sub-figure 8(c)) compared to the boundary of SB (zone 2a and 2b of sub-figure 8(c)). The most translated particles are found near the boundaries of the SB and at the locations of the intersection of shear bands. Hence, an important sign of SB is the presence of a low-velocity particle band surrounded by a high-velocity particle band. Observing the particles' rotation field seems to suggest the opposite. While the magnitude of the particles' rotation field is well correlated with the deviatoric strain field, it can be seen that inside

the SB, location with the most rotated grains is the one with the smallest displacement (zone 1 of sub-figure 8(c,d)). Therefore, correctly predicting SB based on grain kinematics requires taking into account both grain translation and rotation. This remark is also raised by [38] but without giving much detail.

Previous studies in the literature showed that the localisation of deformation can be affected by the level of compaction of granular assembly [26, 39-41]. Comparing now the strain localisation of four samples (Fig. 9) whose responses are presented in Fig. 6.

As we move left to right in Fig. 9, the concentration of shear bands (SB) decreases as the initial void index increases. In the last image, diffuse failure is observed instead of localised failure, indicating a transition from localised to diffuse failure. As the initial void index increase from $e = 0.1982$ to $e = 0.2219$, the width of SB seems to get larger but the magnitude of shear intensity decreases. This is because a denser sample undergoes higher loads and has a higher shear strength and deforms more when entering the softening phase of behaviour. In the case with $e = 0.2614$, the global response shows almost purely contracting behaviour (Fig. 6), diffuse failure is thus obtained. These observations show that the denser the sample, the more obvious the strain localisation phenomenon becomes, and there may be a threshold at which the failure transitions from localised to diffuse. However, determining this threshold for 2D granular assembly is one of the directions for future research.

5 Conclusions

In this paper, by varying a broad range of microscopic parameters, we found an appropriate number of particles for 2D granular assembly that balances the computational cost and mechanical behaviour of granular material. It is recommended to use more than 8100 particles for square granular sample simulated by DEM with multi-periodic boundary conditions. We also explored the effects of interparticle bonding, intergranular friction, and initial void ratios. Our results are in line with previous experimental observations in the literature, showing that the shear strength of granular assembly increases with increasing of intergranular friction and bonding, and with the density of packing.

Finally, we examined macroscopic strain localisation with microscopic effects in terms of static and kinematic aspects; and investigate the shear band formation with regard to the initial density of the sample. It is found that in the case of cohesive-frictional granular materials, (i) the strain localisation displayed by deviatoric strain is in agreement with cohesion-break field. Contacts that lose cohesion are mostly concentrated in the SB and the vicinity of the SB; (ii) in terms of grains kinematic, the occurrence and development of SB correspond to the increasing of field displacement. But it is remarkable to note that grains are less displaced in the core of SB than in the boundary or the vicinity of SB. Nevertheless, grains' rotation shows the opposite observation. The most rotated grains are found in the core of SB. Thus, these two aspects of grain kinematics form an interesting observation/criterion for SB prediction. In the future, further microscopic insight to quantitatively characterized the micro-macro relationship inside SB form should be conducted.

Acknowledgements

This research is funded by Hanoi University of Civil Engineering (HUCE) under grant number 29-2022/KHXD-TĐ.

REFERENCES

[1]- T.-K. Nguyen, J. Desrues, T.-T. Vo, G. Combe, FEM×DEM multi-scale model for cemented granular materials: Inter- and intra-granular cracking induced strain localisation. International Journal for Numerical and Analytical Methods in Geomechanics, 46(5) (2022) 1001-1025. doi:10.1002/nag.3332.

[2]- T.-T. Vo, C.T. Nguyen, T.-K. Nguyen, V.M. Nguyen, T.L. Vu, Impact dynamics and power-law scaling behavior of wet agglomerates. Computational Particle Mechanics, 9(3) (2022) 537-550. doi:10.1007/s40571-021-00427-9.

[3]- H. Wu, A. Papazoglou, G. Viggiani, C. Dano, J. Zhao, Compaction bands in Tuffeau de Maastricht: insights from X-ray tomography and multiscale modeling. Acta Geotechnica, 15(1) (2020) 39-55. doi:10.1007/s11440-019-00904-9.

[4]- J. Zhao, N. Guo, The interplay between anisotropy and strain localisation in granular soils: a multiscale insight. Géotechnique, 65(8) (2015) 642-656. doi:10.1680/geot.14.P.184.

[5]- D. Mašín, C. Tamagnini, G. Viggiani, D. Costanzo, Directional response of a reconstituted fine-grained soil—Part II: performance of different constitutive models. International Journal for Numerical and Analytical Methods in

Geomechanics, 30(13) (2006) 1303-1336. doi:https://doi.org/10.1002/nag.527.
[6]- J. Fonseca, P. Bésuelle, G. Viggiani, Micromechanisms of inelastic deformation in sandstones: an insight using x-ray micro-tomography. Géotechnique Letters, 3(2) (2013) 78-83. doi:10.1680/geolett.13.034.
[7]- A.P. van den Eijnden, P. Bésuelle, F. Collin, R. Chambon, J. Desrues, Modeling the strain localization around an underground gallery with a hydro-mechanical double scale model; effect of anisotropy. Computers and Geotechnics, 85 (2017) 384-400. doi:10.1016/j.compgeo.2016.08.006.
[8]- F.A. Gilabert, J.N. Roux, A. Castellanos, Computer simulation of model cohesive powders: Influence of assembling procedure and contact laws on low consolidation states. Physical Review E, 75(1) (2007) 011303. doi:10.1103/PhysRevE.75.011303.
[9]- C. Liu, Q. Sun, F. Jin, G.G.D. Zhou, A fully coupled hydro-mechanical material point method for saturated dense granular materials. Powder Technology, 314 (2017) 110-120. doi:10.1016/j.powtec.2017.02.022.
[10]- H.H. Bui, G.D. Nguyen, Smoothed particle hydrodynamics (SPH) and its applications in geomechanics: From solid fracture to granular behaviour and multiphase flows in porous media. Computers and Geotechnics, 138 (2021) 104315. doi:10.1016/j.compgeo.2021.104315.
[11]- N. Li, B. Ma, H. Wang, W. Sun, Development of elasto-plastic constitutive model for unbound granular materials under repeated loads. Transportation Geotechnics, 23 (2020) 100347. doi:10.1016/j.trgeo.2020.100347.
[12]- P.A. Cundall, O.D.L. Strack, A discrete numerical model for granular assemblies. Géotechnique, 29(1) (1979) 47-65. doi:10.1680/geot.1979.29.1.47.
[13]- R.K. Pal, R.B. de Macedo, J.E. Andrade, Tunnel excavation in granular media: the role of force chains. Granular Matter, 23(4) (2021) 76. doi:10.1007/s10035-021-01141-2.
[14]- H. Tang, Y. Dong, X. Chu, X. Zhang, The influence of particle rolling and imperfections on the formation of shear bands in granular material. Granular Matter, 18(1) (2016) 12. doi:10.1007/s10035-016-0607-3.
[15]- M.J. Jiang, H.S. Yu, D. Harris, Bond rolling resistance and its effect on yielding of bonded granulates by DEM analyses. International Journal for Numerical and Analytical Methods in Geomechanics, 30(8) (2006) 723-761. doi:10.1002/nag.498.
[16]- T.-K. Nguyen, T.-T. Vo, N.-H. Nguyen, Discrete-element modeling of strain localization in a dense and highly coordinated periodic granular assembly. Frattura e Integrita Strutturale, (59) (2022) 188-197. doi:10.3221/IGF-ESIS.59.14.
[17]- B. Chareyre. Discrete element modeling of composites soil-geosynthetics structures: application to trench anchorages at the top of slopes. Université Joseph-Fourier - Grenoble I, 2003.
[18]- T.K. Nguyen. Multi-scale modeling of cohesive-frictional granular materials. Université de Grenoble, 2013.
[19]- M.R. Kuhn, K. Bagi, Specimen Size Effect in Discrete Element Simulations of Granular Assemblies. Journal of Engineering Mechanics, 135(6) (2009) 485-492. doi:10.1061/(ASCE)0733-9399(2009)135:6(485).
[20]- S. Mohammadi, H. Taiebat, Finite element simulation of an excavation-triggered landslide using large deformation theory. Engineering Geology, 205 (2016) 62-72. doi:10.1016/j.enggeo.2016.02.012.
[21]- N. Guo, L.F. Chen, Z.X. Yang, Multiscale modelling and analysis of footing resting on an anisotropic sand. Géotechnique, 72(4) (2022) 364-376. doi:10.1680/jgeot.20.P.306.
[22]- T.K. Nguyen, A. Argilaga, D. Caillerie, G. Combe, S. Dal Pont, J. Desrues, V. Richefeu, FEMxDEM: a new efficient multi-scale approach for geotechnical problems with strain localization, EDP Sciences. (2017). doi:10.1051/epjconf/201714011007.
[23]- F. Salehnia, F. Collin, X.L. Li, A. Dizier, X. Sillen, R. Charlier, Coupled modeling of Excavation Damaged Zone in Boom clay: Strain localization in rock and distribution of contact pressure on the gallery's lining. Computers and Geotechnics, 69 (2015) 396-410. doi:10.1016/j.compgeo.2015.06.003.
[24]- T.K. Nguyen, G. Combe, D. Caillerie, J. Desrues, FEM × DEM modelling of cohesive granular materials: Numerical homogenisation and multi-scale simulations. Acta Geophysica, 62(5) (2014) 1109-1126. doi:10.2478/s11600-014-0228-3.
[25]- J. Desrues, E. Andò, F.A. Mevoli, L. Debove, G. Viggiani, How does strain localise in standard triaxial tests on sand: Revisiting the mechanism 20 years on. Mechanics Research Communications, 92 (2018) 142-146. doi:10.1016/j.mechrescom.2018.08.007.
[26]- J. Desrues, G. Viggiani, Strain localization in sand: an overview of the experimental results obtained in Grenoble using stereophotogrammetry. International Journal for Numerical and Analytical Methods in Geomechanics, 28(4) (2004) 279-321. doi:10.1002/nag.338.

[27]- W. Wang, J. Pan, F. Jin, Mechanical Behavior of Cemented Granular Aggregates under Uniaxial Compression. Journal of Materials in Civil Engineering, 31(5) (2019) 04019047. doi:10.1061/(ASCE)MT.1943-5533.0002681.
[28]- T.K. Nguyen, G. Combe, D. Caillerie, J. Desrues, Modeling of a cohesive granular materials by a multi-scale approach. AIP Conference Proceedings, 1542(1) (2013) 1194-1197. doi:10.1063/1.4812151.
[29]- G. Combe, J.-N. Roux, Discrete numerical simulation, quasistatic deformation and the origins of strain in granular materials, in Third international symposium on deformation characteristics of geomaterials Lyon, France. (2003). doi:10.48550/arXiv.0901.3842.
[30]- T.-K. Nguyen. On the Representative Volume Element of Dense Granular Assemblies Made of 2D Circular Particles. Singapore: Springer Singapore. (2021), 499-508. doi:10.1007/978-981-16-0945-9_41.
[31]- F. Radjai, Multi-periodic boundary conditions and the Contact Dynamics method. Comptes Rendus Mécanique, 346(3) (2018) 263-277. doi:10.1016/j.crme.2017.12.007.
[32]- Cegeo, B. Saint-Cyr, K. Szarf, C. Voivret, E. Azéma, V. Richefeu, J.Y. Delenne, G. Combe, C. Nouguier-Lehon, P. Villard, P. Sornay, M. Chaze, F. Radjai, Particle shape dependence in 2D granular media. Europhysics Letters, 98(4) (2012) 44008. doi:10.1209/0295-5075/98/44008.
[33]- G. Mollon, A. Quacquarelli, E. Andò, G. Viggiani, Can friction replace roughness in the numerical simulation of granular materials? Granular Matter, 22(2) (2020) 42. doi:10.1007/s10035-020-1004-5.
[34]- J. Desrues, R. Chambon, M. Mokni, F. Mazerolle, Void ratio evolution inside shear bands in triaxial sand specimens studied by computed tomography. Géotechnique, 46(3) (1996) 529-546. doi:10.1680/geot.1996.46.3.529.
[35]- Y. Gao, Q. Chen, Q. Yuan, Y.-H. Wang, The kinematics and micro mechanism of creep in sand based on DEM simulations. Computers and Geotechnics, 153 (2023) 105082. doi:10.1016/j.compgeo.2022.105082.
[36]- K. Bagi, Stress and strain in granular assemblies. Mechanics of Materials, 22(3) (1996) 165-177. doi:10.1016/0167-6636(95)00044-5.
[37]- E. Andò, G. Viggiani, J. Desrues, X-Ray Tomography Experiments on Sand at Different Scales, in Views on Microstructures in Granular Materials, P. Giovine, P.M. Mariano, G. Mortara, Editors. Springer International Publishing: Cham. (2020), 1-20. doi:10.1007/978-3-030-49267-0_1.
[38]- D. Lu, H. Dong, Q. Lin, C. Guo, Z. Gao, X. Du, A method for characterizing the deformation localization in granular materials using the relative particle motion. Computers and Geotechnics, 156 (2023) 105262. doi:10.1016/j.compgeo.2023.105262.
[39]- J. Desrues, R. Chambon, Shear band analysis and shear moduli calibration. International Journal of Solids and Structures, 39(13) (2002) 3757-3776. doi:10.1016/S0020-7683(02)00177-4.
[40]- M. Jiang, W. Zhang, Y. Sun, S. Utili, An investigation on loose cemented granular materials via DEM analyses. Granular Matter, 15(1) (2013) 65-84. doi:10.1007/s10035-012-0382-8.
[41]- P. Bésuelle, J. Desrues, S. Raynaud, Experimental characterisation of the localisation phenomenon inside a Vosges sandstone in a triaxial cell. International Journal of Rock Mechanics and Mining Sciences, 37(8) (2000) 1223-1237. doi:10.1016/S1365-1609(00)00057-5.